

C 13.44:82

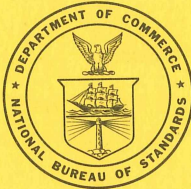
UNIVERSITY OF ARIZONA LIBRARY



3 9001 04297 4140

OGRAPH 82

MICROWAVE IMPEDANCE MEASUREMENTS AND STANDARDS



**U.S. DEPARTMENT OF STANDARDS
NATIONAL BUREAU OF STANDARDS**

UNIVERSITY OF
ARIZONA LIBRARY
Documents Collection

SEP 3 1965

THE NATIONAL BUREAU OF STANDARDS

The National Bureau of Standards is a principal focal point in the Federal Government for assuring maximum application of the physical and engineering sciences to the advancement of technology in industry and commerce. Its responsibilities include development and maintenance of the national standards of measurement, and the provisions of means for making measurements consistent with those standards; determination of physical constants and properties of materials; development of methods for testing materials, mechanisms, and structures, and making such tests as may be necessary, particularly for government agencies; cooperation in the establishment of standard practices for incorporation in codes and specifications; advisory service to government agencies on scientific and technical problems; invention and development of devices to serve special needs of the Government; assistance to industry, business, and consumers in the development and acceptance of commercial standards and simplified trade practice recommendations; administration of programs in cooperation with United States business groups and standards organizations for the development of international standards of practice; and maintenance of a clearinghouse for the collection and dissemination of scientific, technical, and engineering information. The scope of the Bureau's activities is suggested in the following listing of its four Institutes and their organizational units.

Institute for Basic Standards. Applied Mathematics. Electricity. Metrology. Mechanics. Heat. Atomic Physics. Physical Chemistry. Laboratory Astrophysics.* Radiation Physics. Radio Standards Laboratory.* Radio Standards Physics; Radio Standards Engineering. Office of Standard Reference Data.

Institute for Materials Research. Analytical Chemistry. Polymers. Metallurgy. Inorganic Materials. Reactor Radiations. Cryogenics.* Materials Evaluation Laboratory. Office of Standard Reference Materials.

Institute for Applied Technology. Building Research. Information Technology. Performance Test Development. Electronic Instrumentation. Textile and Apparel Technology Center. Technical Analysis. Office of Weights and Measures. Office of Engineering Standards. Office of Invention and Innovation. Office of Technical Resources. Clearinghouse for Federal Scientific and Technical Information.**

Central Radio Propagation Laboratory.* Ionospheric Telecommunications. Tropospheric Telecommunications. Space Environment Forecasting. Aeronomy.

* Located at Boulder, Colorado 80301.

** Located at 5285 Port Royal Road, Springfield, Virginia 22171.

UNITED STATES DEPARTMENT OF COMMERCE • John T. Connor, *Secretary*
NATIONAL BUREAU OF STANDARDS • A. V. Astin, *Director*

Microwave Impedance Measurements and Standards

Robert W. Beatty

National Bureau of Standards
Boulder Laboratories
Boulder, Colorado



National Bureau of Standards Monograph 82

Issued August 12, 1965

For sale by the Superintendent of Documents, U.S. Government Printing Office
Washington, D.C., 20402 - Price 20 cents

Library of Congress Catalog Card No. 65-60054

Foreword

This publication is a tutorial review of microwave impedance measurements and standards. It is not intended to be comprehensive but to emphasize fundamental theory, definitions, the conventional slotted line, and reflectometer techniques. Particular attention is given to discussion of errors.

Sections 1 through 5 provide a theoretical introduction to the subject, which is then followed by detailed discussions of selected measurement techniques and impedance standards. A list of selected references is included.

A. V. ASTIN, *Director.*

Contents

	Page
Foreword.....	III
1. Definition of reflection coefficient.....	1
2. Definition of impedance, normalized impedance.....	2
3. The Smith chart.....	3
4. Effect of change of position of terminal surface.....	5
5. Voltage standing-wave ratio (VSWR).....	6
6. The idealized slotted section.....	7
7. The actual slotted line.....	8
7.1. Irregular variations in probe coupling.....	8
7.2. Probe loading of the slotted line.....	9
a. Probe replaced by shunt admittance, generator nonreflecting.....	9
b. Probe replaced by shunt admittance, arbitrary generator.....	10
c. Three-arm junction representation of slotted line.....	11
7.3. Residual VSWR.....	12
7.4. Other sources of error associated with the slotted line.....	13
a. Change of characteristic impedance by slot.....	13
b. Slot waves.....	13
c. Attenuation or slope.....	14
d. Leakage.....	14
7.5. Still other sources of error.....	14
7.6. Conclusions.....	15
8. Rotating probe devices.....	15
8.1. Rotating probe—rectangular waveguide.....	15
8.2. Rotating probe—coaxial line.....	17
8.3. Rotating probe instruments—other.....	19
9. Resonance lines.....	19
9.1. The Chipman line.....	19
9.2. Squared VSWR response.....	21
10. Reflectometer techniques in general.....	22
10.1. Reflectometer for swept-frequency applications.....	22
10.2. Reflectometer for single-frequency operation.....	23
10.3. Single directional coupler reflectometer.....	23
a. Adjustment of the tuners.....	24
b. Approximate theory of tuning adjustments.....	25
c. “Exact” theory of tuning adjustments.....	27
d. Error analysis.....	29
10.4. Phase of reflection coefficient.....	30
11. Reflection coefficient standards.....	30
12. References.....	32

Microwave Impedance Measurements and Standards

Robert W. Beatty

A survey and discussion of well-known microwave impedance measurement techniques is presented. The discussion includes an introduction [1]¹ which emphasizes basic concepts and reflection coefficient-VSWR relationships. Sources of error in the various measurement techniques are discussed and methods to reduce errors are presented. The discussion of errors in slotted line and reflectometer techniques is most thorough. Methods using rotating loops and resonance lines are included and a brief discussion of microwave impedance standards is given.

1. Definition of Reflection Coefficient

The propagation of electromagnetic energy can generally be regarded as wave propagation.

A particularly simple type of wave is one which travels along a straight line, following a uniform path or waveguide. The wave has sinusoidal time variation at a single frequency and may suffer attenuation due to dissipation but is not reflected unless it encounters some discontinuity in, or termination of, the path or waveguide.

This type of wave is the one to be considered, because other more complicated types can be synthesized by proper combination of appropriate simpler types.

The reflection of a wave traveling in one direction may in general produce a scattering, such that waves in different modes are set up in different directions. However, for our purposes, only the wave coming back along the same path in the same mode is regarded as the reflected wave, the others being regarded as scattered wave components.

If the incident and reflected wave amplitudes are denoted by a and b , respectively, the reflection coefficient is the ratio of b to a . Since the wave amplitudes are usually written in complex form to include phase information regarding the sinusoidal time variation, the reflection coefficient Γ as defined above is, in general, complex.

Thus, it is seen that the concept of reflection coefficient is applied to the case of

- (a) sinusoidal time variation,
- (b) single frequency,
- (c) single propagating mode,

¹ Figures in brackets indicate the literature references at the end of this Monograph.

(d) uniform path or waveguide having a termination or discontinuity which causes reflection, and

(e) incident and reflected waves traveling the same path in opposite directions.

In microwave circuit analysis, it sometimes happens that the waves traveling in opposite directions in a waveguide are not clearly distinguishable as “incident” and “reflected.” One can then make an arbitrary choice and, in doing so, it may be convenient to define certain reflection coefficients as the ratio of b to a and others as the ratio of a to b . This happens because a is often chosen to designate the amplitude of a wave incident on a waveguide junction, and b the amplitude of a wave emerging from the junction.

Thus it may happen that the wave emerging from a junction is the wave incident upon a load. The reflection coefficient of the load would then be the ratio of a to b in this case.

There is no concept of mutual reflection coefficient corresponding to that of mutual impedance. If there were, this would be defined as the ratio of the amplitude of a reflected wave in one mode or path to the amplitude of an incident wave in another mode or path. These ratios are called scattering coefficients rather than reflection coefficients. The concept of reflection coefficients is thus seen to be a special case of the concept of the scattering coefficient.

2. Definition of Impedance, Normalized Impedance

Impedance has been defined as the ratio of v to i , the generalized voltage and current.

If one uses p as a mode index,

$$Z_p = \left(\frac{v_p}{i_p} \right) = \frac{a_p + b_p}{a_p - b_p} \cdot Z_{0p} = \frac{1 + \frac{b_p}{a_p}}{1 - \frac{b_p}{a_p}} \cdot Z_{0p} = \left(\frac{1 + \Gamma_p}{1 - \Gamma_p} \cdot Z_{0p} \right). \quad (1)$$

Conversely,

$$\Gamma_p = \frac{\frac{Z_p}{Z_{0p}} - 1}{\frac{Z_p}{Z_{0p}} + 1}, \quad (2)$$

The characteristic impedance Z_{0p} is a normalization constant whose choice is arbitrary.

One may avoid or hide Z_{0p} by use of the normalized impedance con-

cept. The normalized impedance is

$$NZ_p = \frac{Z_p}{Z_{0p}} = \frac{1 + \Gamma_p}{1 - \Gamma_p} \tag{3}$$

The normalized impedance is a dimensionless ratio, and in common usage the front superscript is dropped. Thus, there may occasionally arise some misunderstanding as to the meaning of Z_p , but this is relatively rare.

3. The Smith Chart

The relationship (2) may be written

$$\Gamma = \frac{Z - 1}{Z + 1},$$

where it is understood that Z represents a normalized impedance for a particular mode. This can be written

$$\Gamma = 1 - \frac{2}{Z + 1} \tag{4}$$

The transformation of lines of constant resistance to circles in the Γ -plane is shown in figure 1.

The transformation corresponding to (4) is shown in simple steps, starting with the dashed line of constant resistance r shown in the

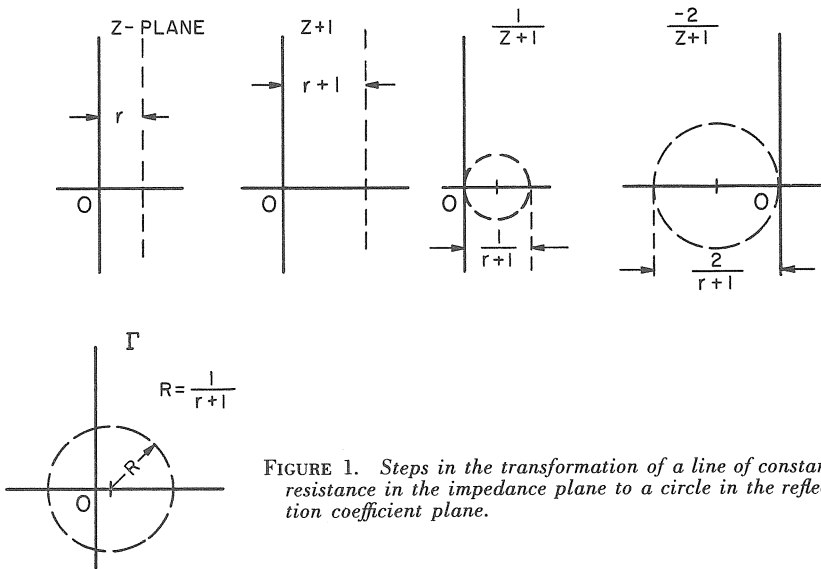


FIGURE 1. Steps in the transformation of a line of constant resistance in the impedance plane to a circle in the reflection coefficient plane.

Z-plane, then in the $Z+1$ plane, then the circle due to inversion, the rotation and stretching caused by multiplication by -2 , and finally the translation caused by the addition of unity.

Note that all lines of constant resistance r transform to circles in the Γ -plane; the circles, having centers which lie on the real axis, have radii equal to the reciprocal of $r+1$ and pass through the point $1, 0$.

A similar development for lines of constant reactance is shown in figure 2.

It is seen that lines of constant reactance transform to circles in the Γ -plane; the circles, having centers which lie on a line perpendicular to the real axis and passing through the point $1, 0$, have radii equal to $\frac{1}{x}$ and pass through the point $1, 0$.

If the transformation of (4) is applied only to portions of lines in the right-half Z -plane, we obtain the familiar Smith chart, shown in figure 3.

The same chart, rotated 180 degrees, can be used to represent the transformation of normalized admittance y to reflection coefficient. This is briefly proved as follows:

$$\Gamma = \frac{1-y}{1+y} = -\left(1 - \frac{2}{y+1}\right), \text{ where } y = g + jb. \tag{5}$$

It is apparent that when y is substituted for Z in (4) we have minus (5), so that the same chart, rotated by 180 degrees, can be used for admittances.

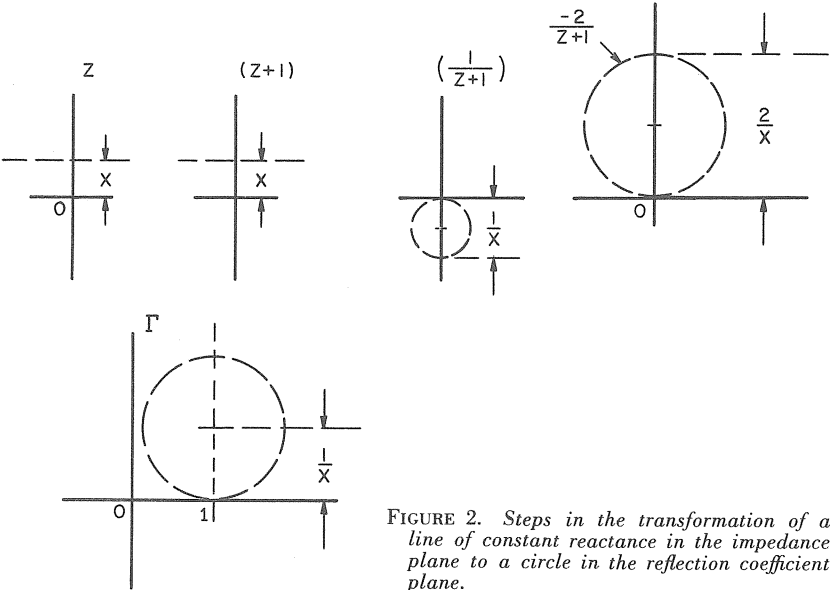
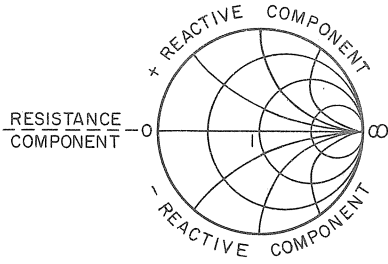


FIGURE 2. Steps in the transformation of a line of constant reactance in the impedance plane to a circle in the reflection coefficient plane.

FIGURE 3. *The Smith Chart.*



4. Effect of Change of Position of Terminal Surface

A change of position of the terminal surface, at which the terminal variables v and i or a and b are determined, changes the reflection coefficient Γ in a simple manner, but the impedance Z is changed in a more complicated way.

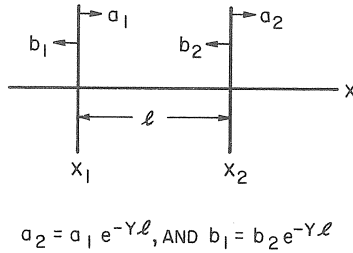


FIGURE 4. *Diagram representing traveling waves on a transmission line as observed at two terminal surfaces having positions x_1 and x_2 .*

The diagram shown in figure 4 applies to the case where Γ_2 is known and we wish to determine Γ_1 at a distance l toward the generator, which is along a uniform waveguide having a propagation constant $\gamma = \alpha + j\beta$.

$$a_2 = a_1 e^{-\gamma l}, \text{ and } b_1 = b_2 e^{-\gamma l}.$$

Therefore,

$$\Gamma_1 = \frac{b_1}{a_1} = \frac{b_2}{a_2} e^{-2\gamma l} = \Gamma_2 e^{-2\gamma l}. \tag{6}$$

The magnitudes are related by

$$|\Gamma_1| = |\Gamma_2| e^{-2\alpha l},$$

and the phase of Γ_1 equals the phase of Γ_2 minus $2\beta l$, or

$$\psi_1 = \psi_2 - 2\beta l + 2n\pi,$$

where n is an integer.

One can derive the conventional transmission line formulas from (6), remembering that

$$\frac{Z}{Z_0} = \frac{1 + \Gamma}{1 - \Gamma}, \text{ and } e^{\gamma l} = \cosh \gamma l + \sinh \gamma l.$$

One obtains

$$Z_1 = \frac{Z_2 + \tanh \gamma l}{1 + Z_2 \tanh \gamma l}, \quad (7)$$

and for the special case of no losses,

$$Z_1 = \frac{Z_2 + j \tan \beta l}{1 + j Z_2 \tan \beta l}. \quad (8)$$

5. Voltage Standing-Wave Ratio (VSWR)

The ratio σ is called the VSWR and may be defined in terms of the reflection coefficient Γ by the equation

$$\sigma = \frac{1 + |\Gamma|}{1 - |\Gamma|}. \quad (9)$$

Accordingly, a VSWR may be associated with any reflection coefficient Γ . If Γ can be determined, the corresponding VSWR can be calculated from (9).

An alternative definition of VSWR requires the postulation of a lossless waveguide in which there is, in general, a standing wave produced by the sum $a + b$ of the incident and reflected waves. This standing wave is $v = a + b$, a standing wave of generalized voltage. As one examines different positions of a terminal surface as it moves along the waveguide, one finds that $v_{\max} = |a| + |b|$, and $v_{\min} = |a| - |b|$. Thus the standing wave ratio of v is

$$\sigma = \frac{|v_{\max}|}{|v_{\min}|} = \frac{|a| + |b|}{|a| - |b|} = \frac{1 + |\Gamma|}{1 - |\Gamma|}. \quad (10)$$

If losses were present (as they always are), then the maxima of v would vary, as would the minima. If we took the ratio of v_{\max} to v_{\min} , where v_{\min} was located approximately one quarter wavelength from the position of v_{\max} , measured toward the generator, then

$$\sigma_A = \frac{|v_{\max}|}{|v_{\min}|} = \frac{|a| + |b|}{|a|e^{\alpha \frac{\lambda_c}{4}} - |b|e^{-\alpha \frac{\lambda_c}{4}}} = \frac{1 + |\Gamma|}{1 - |\Gamma|} e^{-\alpha \frac{\lambda_c}{4}}. \quad (11)$$

One sees that the association of VSWR with a standing wave of v leads to the ratio σ_A of (11), which involves both $|\Gamma|$ and α in a fairly complicated manner. It seems preferable to associate VSWR, σ , with the reflection coefficient Γ as in (9).

6. The Idealized Slotted Section

The propagation of certain waveguide modes is not greatly disturbed if a thin slot is made in the outer conductor of the waveguide in a direction parallel to the axis of the waveguide. Examples of these modes are the TEM mode in coaxial line and the TE_{10} mode in rectangular waveguide.

A probe may be inserted in the slot to sample the fields, and movement of the probe along the slot will provide data on the variation of the field strength as a function of axial length.

Probes may sample either the electric or the magnetic field, or both, and may sample either transverse components, axial components, or both. The usual type of probe encountered in commercially available instruments is one which samples the transverse component of the electric field and does not respond to the magnetic field or to axial components of the electric field (if present).

Ideally, the output level $|b_3|$ of the probe to the detector is proportional to the strength of the field sampled. For example, if the transverse component \mathbf{E}_t of the electric field is sampled,

$$|b_3| = K_1 |\mathbf{E}_t| = K_2 |V| = K_2 |a + b| = K_2 |a| \cdot |1 + \Gamma|, \quad (12)$$

where K_1 and K_2 are constants. Thus, the probe samples the standing wave which is set up as the sum of the oppositely directed traveling waves having amplitudes a and b .

Suppose that the probe is located at terminal surface 1, whose position is variable, and the load (Γ_2) is at terminal surface 2, whose position is fixed. With reference to the diagram of section 4, the probe output level is

$$|b_3| = K_2 |a_1| \cdot |1 + \Gamma_1| = K_2 |a_2| e^{\alpha l} \left| 1 + |\Gamma_2| e^{j(\psi_2 - 2\gamma l)} \right|. \quad (13)$$

In the idealized slotted line, which is lossless ($\gamma = j\beta$, $\alpha = 0$),

$$|b_3| = K_2 |a| \cdot \left| 1 + |\Gamma_L| e^{j(\psi_L - 2\beta l)} \right|. \quad (14)$$

The corresponding vector diagram is shown in figure 5. As the probe changes position, the smaller of the two vector components rotates, and goes in and out of phase with the fixed vector component of unit magnitude.

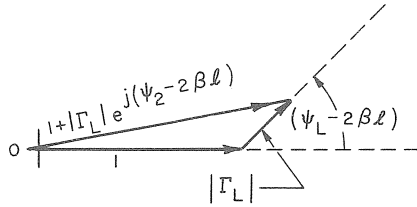


FIGURE 5. Vector diagram pertinent to the probe output of an idealized slotted line.

Thus the ratio of maximum to minimum probe output is

$$\frac{|b_3|_{\max}}{|b_3|_{\min}} = \frac{1 + |\Gamma_L|}{1 - |\Gamma_L|} = \sigma_L \text{ (the VSWR).} \quad (15)$$

One sees from the diagram that as the probe moves in a direction away from the load, the first minimum in its output occurs when

$$\psi_L - 2\beta l_m = \pm \pi. \quad (16)$$

The phase angle ψ_L of the reflection coefficient of the load is then given by

$$\psi_L = 2\beta l_m \pm \pi. \quad (17)$$

7. The Actual Slotted Line

Although the idealized slotted line is simple, any actual slotted line is quite complicated, and a rigorous analysis of its performance is quite difficult. Errors due to unavoidable mechanical irregularities in the construction of slotted lines have never been reduced to the point where the complexity of a rigorous analysis was justified. Steps have been taken in the direction of a more rigorous analysis of actual slotted line behavior, but these have found relatively little application in practice.

Sources of error will be listed, and some of them will be discussed in more or less detail in the following paragraphs.

7.1. Irregular Variations in Probe Coupling

The irregular variations in probe coupling caused by unavoidable mechanical defects in the construction will cause corresponding variations in the probe output. These unwanted variations are superimposed on the cyclical variations due to the standing wave, and they will cause the observed standing wave ratio to differ from the actual standing wave ratio. They may even mask the variation that one wishes to observe, and this occurs approximately when the limits of variation are the same.

For example, if the irregular variations in probe output have a maximum amplitude of ± 0.5 percent (a typical value for precision slotted lines of high quality), they may begin to mask the cyclical variations from a load having a VSWR of 1.01, or less.

These irregular variations are most probably caused by variations in the penetration of the probe in the slot as the probe and detector move in an axial direction. Irregular transverse motions of the probe within the slot will also contribute. Irregularities in the inside dimensions of the waveguide will also cause irregular variations in probe output but will probably contribute less than the above causes.

A less obvious but often troublesome source of irregular variations in probe output is the variation in contact resistance between the probe carriage and the slotted line. This contact resistance is in series with the rf current that flows into the probe circuit from the waveguide.

7.2. Probe Loading of the Slotted Line

An important source of error in slotted line measurements is the probe loading effect. In the ideal situation, the probe is decoupled so as to penetrate the waveguide only very slightly, and hence it does not disturb the fields within the waveguide.

In practice, however, one must have sufficient coupling so that enough energy is extracted from the waveguide to operate the measuring or indicating apparatus. As a practical approach to this problem, it is recommended that one begin with more than adequate probe insertion and note the change in observed VSWR as one gradually, in small increments, withdraws the probe. When the change in VSWR has become negligible, the probe has been sufficiently decoupled.

One might like to be able to estimate the error caused by probe loading and obtain quantitative results. In some cases, it might even be desirable to operate with a deeply inserted probe and make corrections for the probe loading effects. These problems have been solved, but the solutions have not been reduced to practice except in restricted cases, for example, when it is assumed that the generator is nonreflecting.

Several analyses have been made, each progressively more rigorous than the other. However, with more rigor comes greater complexity, and the need must be great before the results of a rigorous analysis are applied to a simple measurement.

In the following, three analyses will be briefly discussed.

a. Probe Replaced by Shunt Admittance, Generator Nonreflecting

One analysis has been made by assuming that the probe dimensions are small compared with a wavelength and that its effect on the waveguide is that of a shunt admittance. In order to simplify the analysis, it has also been assumed that the generator is nonreflecting.

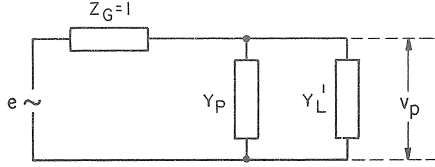


FIGURE 6. *Simplified equivalent circuit of a slotted line for analysis of probe loading effects.*

We can then draw a simple equivalent circuit as shown in figure 6. In this circuit, normalized impedances and admittances are used, and the circuit is assumed to represent conditions at a terminal surface in the waveguide located at the probe position. The admittance Y_L' is related to the actual load admittance by (7), if one replaces Z_1 by $\frac{1}{Y_L}$ and Z_2 by $\frac{1}{Y_L}$. It is assumed that there are no losses in the waveguide.

The expression for v_p is

$$v_p = e \frac{\frac{1}{Y_p + Y_L'}}{1 + \frac{1}{Y_p + Y_L'}} = \frac{e}{1 + Y_p + Y_L'}. \quad (18)$$

It is assumed that the probe output level $|b_3|$ is proportional to $|v_p|$, so that the above equation gives the probe response.

In the ideal situation, $Y_p = 0$, and

$$|b_3| = \frac{k}{1 + Y_L'} = \frac{k}{2} (1 + \Gamma_L'), \quad (19)$$

where k is a constant. This is similar to (12), and the ideal response is obtained. However, the effect of the probe admittance Y_p is to modify the probe response so that the observed ratio of maximum to minimum is no longer equal to the VSWR, and the distance to the first minimum no longer gives ψ_L by calculation from (17).

Corrections to these observed values have been calculated and some information on them is given by Ginzton [2]. One must know Y_p in order to apply these corrections. It is difficult to calculate Y_p or to measure it, but this need not be done, since it can be obtained by analysis of the response curve [3].

b. Probe Replaced by Shunt Admittance, Arbitrary Generator

If one desires a little more rigor and takes into account the fact that the generator may not be matched to the waveguide, the analysis becomes a bit more complicated in that one more variable, Y_G , the generator admittance, is involved.

Following the same procedures used to obtain (18), we now obtain, taking into account Y_G ,

$$v_p = e' \frac{Y'_G}{Y'_G + Y_p + Y'_L} = \frac{2b_G}{1 + \Gamma'_G} \cdot \frac{1}{Y'_G + Y_p + Y'_L}, \quad (20)$$

where b_G is the amplitude of the wave emerging from the generator when it is terminated by a nonreflecting load.

In the above equation, the prime indicates that the quantity indicated is referred to the terminal surface located at the probe position.

Since (20) is similar to (18), it is to be assumed that a similar distortion of the probe response occurs, but this distortion is a little more complicated and the analysis has not been carried as far, mainly because of the difficulties one would have in graphically presenting the results. If one knows Y_G and Y_p , it is possible to determine their effect on the probe response from (20). However, the more practical problem, that of finding Y_L given the probe response, Y_G and Y_p , has not been solved at present.

It should be noted that the foregoing analyses may take simpler forms if the probe loading is small. It can then be assumed that reflections by the probe interact with reflections by the generator and the load, going in and out of phase with each other as the probe changes position.

It is also interesting to observe that, even when the load is nonreflecting ($Y'_L = 1$), one can observe a VSWR if $Y_G \neq 1$. This observed VSWR is not related to the load in any way, however.

c. Three-Arm Junction Representation of Slotted Line

If more rigor is desired, the slotted line may be considered as a three-arm waveguide junction as shown in figure 7.

This approach is necessary if the probe dimensions are not small compared to a wavelength or cannot, for some other reason, be represented by a simple admittance shunted across the waveguide.

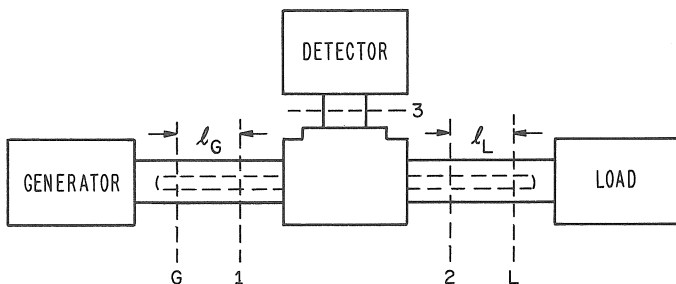


FIGURE 7. Representation of a slotted line as a three-arm waveguide junction.

D. M. Kerns has obtained the characteristic equation giving the detector response for this case [4]. The equation is as follows:

$$b_3 = \frac{c e^{-j\beta l_G}}{1 + Y_p + m\Gamma_G e^{-j2\beta l_G} + [1 + n\Gamma_G e^{-j2\beta l_G}]Y(K\Gamma_L, \beta l_L)}, \quad (21)$$

where

$$Y(K\Gamma_L, \beta l_L) = \frac{1 - K\Gamma_L e^{-j2\beta l_L}}{1 + K\Gamma_L e^{-j2\beta l_L}}$$

and c , Y_p , m , n , and K are constants independent of l_G and l_L .

It is worth noting that four characteristic constants, Y_p , $m\Gamma_G$, $n\Gamma_G$, and K , are associated with the characteristic equation, instead of only two, Y_G and Y_p , as before. If the generator is matched to the waveguide, two of these constants vanish, and if the junction is lossless, $|K|=1$. In this case, (21) reduces to the same form as (18).

Further analysis has not been performed but could be completed if desired. The practical problem is to obtain the reflection coefficient of the load given the response curve of the detector and any additional data that are required, such as the four characteristic constants above.

7.3. Residual VSWR

The residual VSWR of a slotted line is the VSWR within the slotted section when the load is nonreflecting. It is caused by reflections from discontinuities such as occur at the end of the slot, at tapered sections, at beads which support the center conductor (when used), and at connectors.

All of these reflections add to the reflection from the load, and since the phase difference is usually unknown, this represents a source of error.

Assuming that the residual reflection coefficient Γ_r corresponding to the residual VSWR is small, as is usually the case, one can write

$$\Gamma \approx \Gamma_r + \Gamma_L, \quad (22)$$

where Γ is the reflection coefficient in the slotted line, and Γ_L is the reflection coefficient of the load. If only the magnitudes are known, we can say that

$$|\Gamma| - |\Gamma_r| \leq |\Gamma_L| \leq |\Gamma| + |\Gamma_r|. \quad (23)$$

For example if the residual VSWR is 1.04 ($|\Gamma_r| \approx 0.02$) and the VSWR in the slotted line is 2.50 ($|\Gamma| \approx 0.429$), the VSWR of the load is between 2.38 and 2.63 ($0.409 \leq |\Gamma_L| \leq 0.449$).

It should be noted that the choice of terminal surface at which Γ_L is to be specified is somewhat arbitrary and that the residual VSWR is then also somewhat arbitrary. For example, the terminal surface can be chosen on either side of the connector. In one case the reflection from the connector would be included in the residual VSWR, and in the other case it would not.

7.4. Other Sources of Error Associated With the Slotted Line

A number of other sources of error as follows are associated with the slotted line, and while these normally produce negligible errors in well-designed apparatus, one cannot always assume that they are negligible.

a. Change of Characteristic Impedance by Slot

In general, the characteristic impedance of the slotted waveguide is different from that of the unslotted portions at the ends. The normalized impedance one measures is thus referred to a base other than the desired one.

However, the error caused by this source is usually far less than that from the other sources and may be neglected. In case of a very wide slot, however, it may be desirable to check this source. The increase in characteristic impedance in ohms caused by a slot in a coaxial line, TEM mode is

$$\Delta Z_0 \leq 0.03\theta^2, \quad (24)$$

where θ is the angular opening of the slot in radians. A slot opening of 0.1 rad (5.73 deg) will produce an impedance change of less than 0.0003 ohms, for example [5].

b. Slot Waves

The presence of the slot makes possible the propagation of modes other than those which propagate in an unslotted waveguide. These can be excited by the discontinuities at the ends of the slot or by asymmetrical location or construction of the slot as well as by the probe. At certain frequencies, a slot mode may resonate, increasing its strength and effect. If the probe responds to the fields in the slot mode, its response will be distorted and errors produced. The presence of slot waves may sometimes be observed as this distortion effect, but sometimes their presence is unnoticed.

They can be reduced by tapering the ends of the slot, symmetrical construction and location of the slot, and damping of the resonances by judicious placement of absorbing material.

A simpler and more accurate expression for the limits of VSWR of σ_L , the VSWR of the load, is $\frac{\sigma}{\sigma_r} \geq \sigma_L \geq \sigma \sigma_r$, where σ is the resid VSWR observed in the slotted (667-763 0-65-3) line, and σ_r is the residual VSWR. It is not required that $|\Gamma_r|$ be small for this expression to hold exactly in the lossless case. In the above example, this gives $2.40 \geq \sigma_L \geq 2.60$.

← errata



c. Attenuation or Slope

In any slotted line, the amplitude of the standing wave decays because of losses as one proceeds in an axial direction. Thus, one maximum is not as large as the next one. If the ratio is taken of two maxima to the minimum response between them, slightly different results will be obtained. This effect is described by (11).

If the attenuation is small, as is usually the case, this effect may be neglected, especially if one takes the average of the two ratios mentioned above. If one denotes the average by r , the VSWR (σ_L) of the load is approximately

$$\sigma_L \approx r \left[1 + \alpha l \left(r - \frac{1}{r} \right) \right], \quad (25)$$

where α is the attenuation in nepers per unit length and l is the distance from the terminal surface of the load to the probe position for minimum response.

d. Leakage

Leakage to the detector from the slot or from end connectors of the slotted line may cause difficulty in cases where the probe is decoupled and the detector has high gain. It can cause errors in the measured ratio of maximum to minimum response.

7.5. Still Other Sources of Error

A number of other sources of error can be mentioned. Some are normally small, while others require special precautions in order to keep them small.

Appreciable harmonic content or spurious modulation of the signal source can cause large errors. Pulling of the oscillator caused by variations in loading as the probe changes position can be troublesome. Instability and noise, both in the signal source and the detector, can cause errors. The apparatus used for measuring ratios can contribute to error if not accurate. The solutions to these possible sources of trouble are fairly obvious.

Measurement of the phase angle of reflection coefficient or impedance is subject to many sources of error, such as error in measuring the displacement of the probe, error in measuring frequency, difference in wavelength in the slotted and unslotted portions of the waveguide, probe loading effects, etc.

7.6. Conclusions

The slotted line is a convenient instrument to use and measurements can be made of VSWR and phase angle of reflection coefficient with fair to good accuracy.

However, the possibilities for making errors are many, and a skilled operator is a valuable accessory. The nature of the error sources is such that the refinement of slotted lines for highly accurate measurements is difficult and expensive. It has been found that the tuned single directional coupler reflectometer to be described has more promise for single-frequency operation.

Due to convenience of operation, reasonable size, ease of obtaining phase information, ease of retuning when changing frequency, rapidity of measurement, etc., the slotted line is the most popular instrument for measuring reflection coefficient and impedance at microwave frequencies. However, its refinement for measurements of higher accuracy appears to be unprofitable.

8. Rotating Probe Devices

Instead of sliding a probe which couples to the electric field in an axial slot to make a measurement of reflection coefficient, one can obtain a similar response and make similar measurements with a rotating probe which couples to the magnetic field.

Two versions will be described, one for rectangular waveguide and one for coaxial line.

8.1. Rotating Probe – Rectangular Waveguide

The rotating probe is located in the top or broad wall of the waveguide, off center, where the axial and transverse components of the magnetic field for the dominant mode have equal magnitudes. This can be shown to occur when $x = d$, and

$$d = \frac{a}{\pi} \tan^{-1} \frac{\lambda_G}{\lambda_c}, \quad (26)$$

where λ_G is the guide wavelength, λ_c is the cutoff wavelength, and x , d , and a are shown in the diagram of figure 8.

The two components of the magnetic field in a progressive wave traveling in the Z -direction are, at $x = d$, not only equal in magnitude, but are at right angles in space and in time quadrature. These conditions produce a circularly polarized magnetic field which can be coupled out by a circular waveguide placed as shown. The diameter of the circular waveguide is such that it is below cutoff for the dominant mode.

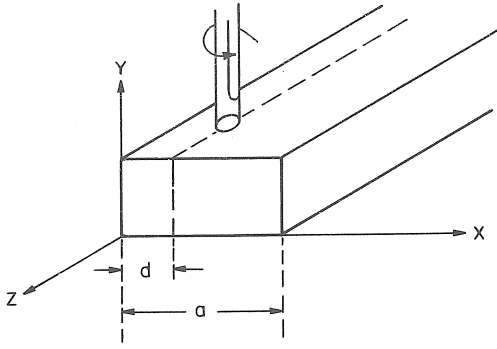


FIGURE 8. Rotating probe coupling to magnetic fields in a rectangular waveguide.

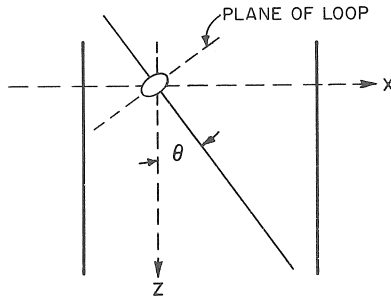


FIGURE 9. Orientation of coupling loop relative to axis of waveguide.

This results in low probe loading of the rectangular waveguide, which is desirable.

The effect of a reflected wave traveling in the opposite direction in the rectangular waveguide is to couple out a circularly polarized component having opposite rotation. The result is an elliptically polarized wave in the circular waveguide. Rotation of the probe will give a cyclically varying output similar to the slotted line response, except that angular displacement takes the place of linear displacement.

It can be shown that

$$H_x = jH_0(1 - |\Gamma_L|e^{j\psi_L}),$$

and

$$H_z = H_0(1 + |\Gamma_L|e^{j\psi_L}), \quad (27)$$

where $H_0 = \beta \frac{\pi}{a} A \sin \frac{\pi d}{a}$, and A is an amplitude factor.

The coupling loop is oriented as shown in figure 9.

The output level $|b_p|$ of the coupling loop is

$$\begin{aligned} |b_p| &= K |H_z \cos \theta + H_x \sin \theta| \\ &= KH_0 |1 + |\Gamma_L| e^{j(\psi_L - 2\theta)}|. \end{aligned} \quad (28)$$

This is of the same form as (14), showing that θ plays the same role in this instrument that βl plays in the slotted line. The procedure to measure Γ_L is, therefore, similar to that used with the slotted line, if one substitutes rotation for linear displacement.

Since the correct location of the probe varies with frequency, one would expect errors to be introduced when not operating at the design frequency. Probe loading effects would be present but differing from those in the slotted line. Some error might be expected if the probe couples to the electric as well as the magnetic fields. Any axial variation of the probe during rotation will cause error. However slot effects have been avoided. A detailed description of an actual instrument is given by Hopfer and Nadler [6].

Although this instrument is commercially available in some waveguide sizes, it has not yet replaced the slotted line in popularity.

8.2. Rotating Probe—Coaxial Line

In coaxial line, an instrument using a rotating probe coupled to the magnetic field has been developed and is commercially available. Such an instrument operates below 1 GHz (Gc/s) and at these frequencies is smaller than a slotted line and has comparable accuracy.

As shown in the diagram of figure 10, it consists of a coaxial tee junction with a circular waveguide, below cutoff, coupled at the branch point.

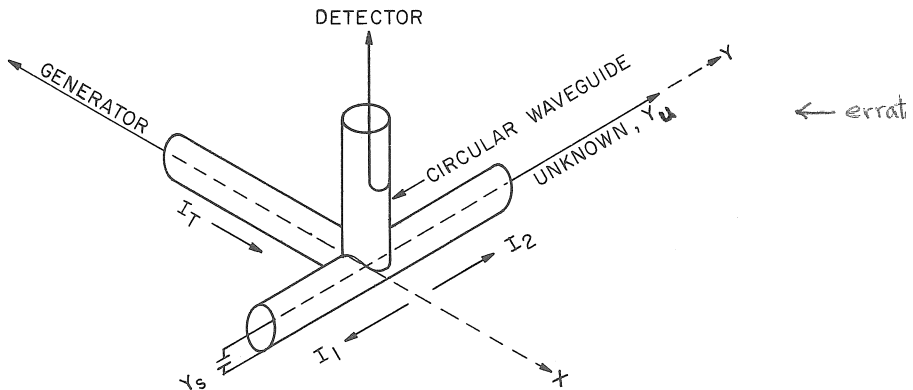


FIGURE 10. Diagram of a standing wave indicator for coaxial line.

The rotating probe is located within the circular waveguide incorporating a mode filter so as to permit coupling only to the magnetic field and not to the electric field.

In deriving the working equation of the instrument, it is assumed that the transverse magnetic field components of the $TE_{1,1}$ mode in the circular waveguide are excited by, and have magnitudes proportional to, the branch currents I_T , I_1 , and I_2 . One can then write

$$\begin{cases} H_x = C_1(I_2 - I_1) \\ H_y = C_2 I_T. \end{cases} \quad (29)$$

errata


Referring the unknown admittance Y_u and that of the standard Y_s to the branch point, and denoting these referred admittances by primes, we have

$$\begin{cases} H_x = C_1 v (Y'_u - Y'_s) \\ H_y = C_2 v (Y'_u + Y'_s), \end{cases} \quad (30)$$

where v is the voltage at the branch point.

The output level, denoted by $|b_p|$, of the probe (coupling to the magnetic field, and having an angular position θ as shown in figure 11) is

$$|b_p| = K |H_x \sin \theta - H_y \cos \theta|. \quad (31)$$

If one assumes that $C_1 = C_2 = C$, and that $Y'_s = -jY_0$, where Y_0 is the characteristic admittance of the coaxial line, it can be shown that

↳

$$|b_p| = \frac{K C v Y_0 \sqrt{2}}{|1 + \Gamma'_u|} \cdot \left| 1 + |\Gamma'_u| e^{j(\psi'_u - \frac{\pi}{2} + 2\theta)} \right|. \quad (32)$$

This is of the same form as (14), showing that $(\theta - \frac{\pi}{4})$ in this instrument plays the same role that βl does in the slotted line. The measurement technique is then analogous and needs no further discussion.

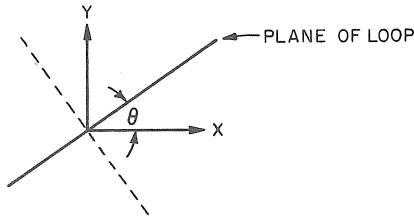


FIGURE 11. Orientation of coupling loop relative to axes of coaxial lines.

Errors will result from inability to satisfy the assumptions made in deriving (32), but, below 1 GHz, these errors can be kept small. A detailed description of an actual instrument is given by Hopfer and Finke [7].

8.3. Rotating Probe Instruments—Other

Other instruments using rotating probes have been developed [8] in which the principle of operation is similar to, or a variation on, those described above.

9. Resonance Lines

Microwave impedance measurements may be made by observing resonance phenomena produced by sliding short-circuiting plungers or otherwise varying susceptances of coaxial lines and other types of uniform cylindrical waveguide.

9.1. The Chipman Line

An early resonance line technique was developed by R. A. Chipman [9], and refined by Meier and Summers [10].

This technique is characterized by a response which is the inverse of that from a slotted line, and both generator and probe are loosely coupled to the waveguide (which is often a coaxial line).

As shown in the diagram of figure 12, the generator is loosely coupled to the waveguide at a fixed position, while the detector is loosely coupled to respond to the current in a sliding short-circuit. Measurements are made by sliding the short-circuit and observing the detector response curve. A simplified analysis based upon an idealized model yields the equations of basic interest. It is convenient and appropriate to assume that the line is lossless, that the generator coupling intro-

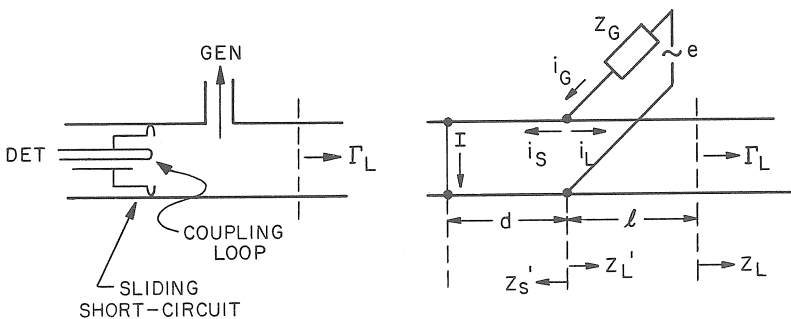


FIGURE 12. Diagram and simplified equivalent circuit for a form of resonance line developed by Chipman.

duces no discontinuity and does not appreciably load the line, and that $|Z_G|$ is great enough so that i_G may be considered constant.

The current on a short-circuited lossless line is known to be sinusoidally distributed, or

$$i_s = I \cos \beta d.$$

From Kirchhoff's law,

$$\begin{aligned} i_G &= i_s + i_L \text{ or } i_s = i_G - i_L, \\ I &= \frac{i_G - i_L}{\cos \beta d}. \end{aligned}$$

However, from elementary circuit theory,

$$i_L = e \frac{Z_p}{Z_G + Z_p} \cdot \frac{1}{Z'_L} = i_G \frac{Z_p}{Z'_L},$$

where

$$Z_p = \frac{1}{\frac{1}{Z'_S} + \frac{1}{Z'_L}}.$$

The amplitude of the probe output is proportional to

$$I = \frac{i_G}{\cos \beta d} \left(1 - \frac{Z_p}{Z'_L} \right) = \frac{i_G}{\cos \beta d} \cdot \frac{1}{\frac{Z'_S}{Z'_L} + 1}.$$

This equation yields the response, but it is desirable to convert to another form in which d and l are explicitly involved. Replacing Z'_S and Z'_L by their corresponding reflection coefficients Γ'_S and Γ'_L , where $\Gamma'_S = \Gamma_S e^{-j2\beta d}$, and $\Gamma'_L = \Gamma_L e^{-j2\beta l}$,

$$I = i_G \left(\frac{1 - \Gamma_S e^{-j2\beta d}}{1 + e^{-j2\beta d}} \right) (1 + \Gamma_L e^{-j2\beta l}) \frac{e^{-j\beta d}}{1 - \Gamma_S \Gamma_L e^{-j2\beta(d+l)}}. \quad (33)$$

Assuming that the detector is loosely coupled to a perfect short-circuit ($|\Gamma_S| = 1$), and that d is the independent variable, the observed ratio r of maximum to minimum probe output level is

$$r = \frac{1 + |\Gamma_L|}{1 - |\Gamma_L|} = \sigma_L, \text{ the VSWR.} \quad (34)$$

Usually l is less than one quarter wavelength, and the first maximum probe output as d increases from zero occurs when

$$\psi_L - 2\beta(d_m + l) = \pm \pi,$$

or

$$\psi_L = 2\beta(d_m + l) \pm \pi. \quad (35)$$

Instruments based upon this principle are not commercially available but have been constructed for special applications. Such instruments are mechanically more awkward than slotted lines, have greater loss between generator and detector, and afford little or no increase in accuracy because it is difficult to maintain constant probe coupling. The absence of a slot is an advantage and the inverse response is useful in special applications such as the determination of the line attenuation. In order to make accurate measurements, the assumptions made in deriving (33) have to be satisfied, and the reflection coefficient Γ_S of the short-circuit has to be determined. In addition, great care is needed in the design and construction of the line, insuring its uniformity and the constancy of the detector probe coupling.

9.2. Squared VSWR Response

It is interesting to consider the response from another type of resonance line having fixed probes and variable short-circuit. Referring to a diagram and model, as shown in figure 13, and making simplifying assumptions as above, a simple equation may be derived for the response.

We assume that the detector is coupled to respond to v and that d is now fixed while l or ψ_L is variable. In a manner similar to before,

$$v = e \frac{Z_p}{Z_G + Z_p} \approx i_G Z_p = \frac{i_G}{\frac{1}{Z'_S} + \frac{1}{Z'_L}}$$

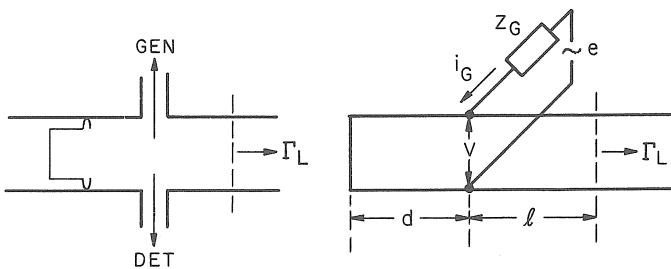


FIGURE 13. Diagram and simplified equivalent circuit of a form of resonance line which can have squared VSWR response.

If $d = \frac{\lambda_G}{4}$, $Z'_S = \infty$ (lossless case), and

$$v = i_G Z'_L = i_G \frac{1 + |\Gamma_L| e^{j(\psi_L - 2\beta l)}}{1 - |\Gamma_L| e^{j(\psi_L - 2\beta l)}}. \quad (36)$$

As either ψ_L or l is varied, the ratio r of $|v|_{\max}$ to $|v|_{\min}$,

$$r = \left(\frac{1 + |\Gamma_L|}{1 - |\Gamma_L|} \right)^2 = \sigma_L^2. \quad (37)$$

As l is increased, the first minimum $|v|$ occurs when $\psi_L - 2\beta l_m = \pm \pi$, so that

$$\psi_L = 2\beta l_m \pm \pi. \quad (38)$$

It is interesting to note that squared VSWR response [11] may be obtained from other arrangements than the one shown.

10. Reflectometer Techniques in General

It is commonly understood that a reflectometer is an instrument used to determine the magnitude $|\Gamma|$ of the reflection coefficient, or the corresponding VSWR. Phase information is usually not provided, but can be obtained by appropriate modifications of the instruments and techniques.

10.1. Reflectometer for Swept-Frequency Applications

One form of reflectometer widely used for swept-frequency measurements consists of two directional couplers connected as in the diagram of figure 14.

The detectors D_I and D_R couple loosely to the incident and reflected waves, respectively, so that the ratio of their input levels ideally equals $|\Gamma_L|$, the magnitude of the reflection coefficient of the load. Ratio meters have been developed to make this a direct-reading instrument, which

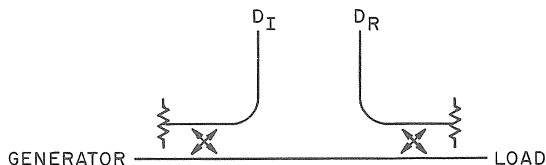


FIGURE 14. Simple diagram of conventional reflectometer.

is calibrated by replacing the load by a short-circuit, and adjusting the detectors and ratio meter to indicate $|\Gamma|=1$. In addition to the advantage of covering a broad frequency range with little or no adjustment, this form of reflectometer is relatively insensitive to amplitude changes of the generator such as those associated with instability.

In order to obtain best accuracy, the directional couplers should have high directivity, loose coupling, and excellent VSWR characteristics. In addition, the generator as seen at the plane of connection of the load should be essentially non-reflecting over the frequency band [12].

With equipment presently commercially available, one can expect to make measurements of $|\Gamma_L|$ over the range 0.1 to 0.35 with an uncertainty of less than 5 percent at frequencies up to 140 GHz.

10.2. Reflectometer for Single-Frequency Operation

Methods have been developed [12] for reducing errors in reflectometer measurements caused by imperfect directivity and multiple reflections between load and generator by use of auxiliary tuners placed as shown in figure 15.

The tuners are carefully adjusted before making a measurement. The adjustment [12] is such as to make the ratio of the detector output levels very closely proportional to $|\Gamma_L|$. It is possible, also, to estimate the limits of error caused by imperfect adjustment of the tuners from data obtained during the adjustment process.

By this technique, one obtains improved accuracy at the sacrifice of swept frequency operation and ease of operation, since the tuning adjustments can be tedious. The measurement remains insensitive to changes in level of the generator, however.

10.3. Single Directional Coupler Reflectometer

If a stable generator is available, the use of a single directional coupler with two tuners will permit accurate measurements at a single frequency, and reduces the number of tuners to be adjusted. Instead of simultaneously observing the ratio of two detector outputs, one alternately connects the unknown and then a standard of reflection coefficient at

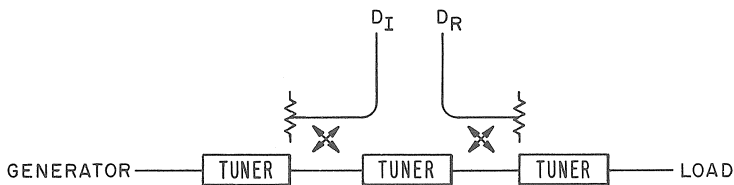


FIGURE 15. Diagram showing the addition of tuners to a conventional reflectometer to improve its performance for single-frequency operation.

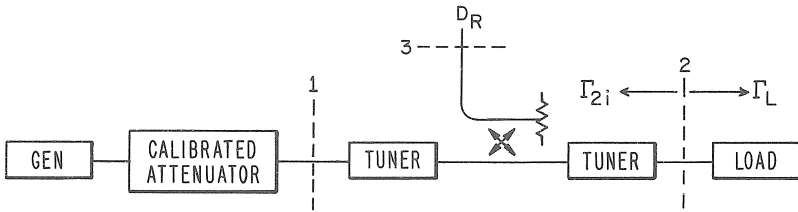


FIGURE 16. Simple schematic diagram of a tuned, single-directional coupler reflectometer.

the plane of the load. A calibrated attenuator is used to return the detector output to the same value, and the ratio of levels can be read from the attenuator dial.

The arrangement of apparatus is as shown in figure 16.

Ideally, the change in attenuation ΔA under the above conditions equals the change in return loss when the unknown load $|\Gamma_u|$ is substituted for the standard $|\Gamma_s|$. This is expressed as

errata →

$$\Delta A = 20 \log_{10} \frac{|\Gamma_s|}{|\Gamma_u|}. \quad (39)$$

In the special but usual case in which a short circuit is used as the standard, and the attenuator is initially set on zero,

↳

$$A = 20 \log_{10} \frac{1}{|\Gamma_u|}. \quad (40)$$

Tables of return loss [13, 14] are available to facilitate the determination of $|\Gamma_u|$ once A has been measured.

errata →

a. Adjustment of the Tuners

The purpose of adjusting the tuners [15] is to obtain two conditions, (a) infinite directivity, and (b) elimination of multiple reflections at the plane of the load. It will be shown later that achievement of these two conditions will result in ideal behavior of the reflectometer, in that the side arm output level will be proportional to $|\Gamma_L|$.

Infinite directivity would be obtained if the side arm output were zero when the load was nonreflecting. In principle, one could connect a nonreflecting load and adjust the tuner near the load until the side arm output was reduced to zero. In practice, however, it is difficult to obtain a load having no reflection, and another method is recommended.

Referring to the above diagram, it is assumed that there is a section of waveguide between the load and the tuner, and that this is sufficiently long so that one can slide a termination within it for a distance of at least one-quarter wavelength. This waveguide section is attached to the tuner and is regarded as a part of the reflectometer.

A termination having a low reflection, for example VSWR less than 1.02, is slid back and forth in this waveguide and one observes cyclical

variations in the level of the side arm output. The adjacent tuner is then adjusted until these cyclical variations have been eliminated or reduced to a low amount, say ± 0.5 dB.

The adjustment of the other tuner then follows in a similar way except that instead of using a sliding termination having a low reflection, one slides a short-circuit, and instead of adjusting to a limit of ± 0.5 dB, one does not stop adjusting until the cyclical variation in the side arm output is less than ± 0.01 dB. This second adjustment will satisfy or closely approximate the second condition mentioned above, in which multiple reflections at the plane of the load are eliminated. In figure 16, this condition implies that $\Gamma_{2i} = 0$ at the plane $\mathcal{E}l$.

← errata

b. Approximate Theory of Tuning Adjustments

It can be shown that the amplitude b_3 of the emergent wave from the side arm of the directional coupler may be written [1] in the form

$$b_3 = C \frac{1 + K\Gamma_L}{1 - \Gamma_{2i}\Gamma_L}, \quad (41)$$

where

$$C = \frac{S_{31}b_G}{\begin{vmatrix} (1 - S_{11}\Gamma_G) & S_{13}\Gamma_L \\ S_{31}\Gamma_G & (1 - S_{33}\Gamma_D) \end{vmatrix}},$$

$$K = \frac{\begin{vmatrix} S_{21}S_{22} \\ S_{31}S_{32} \end{vmatrix}}{S_{31}},$$

d

$$\Gamma_{2i} = \frac{\begin{vmatrix} -(1 - S_{11}\Gamma_G) & S_{12} & S_{13}\Gamma_D \\ S_{21}\Gamma_G & S_{22} & S_{23}\Gamma_D \\ S_{31}\Gamma_G & S_{32} & -(1 - S_{33}\Gamma_D) \end{vmatrix}}{\begin{vmatrix} (1 - S_{11}\Gamma_G) & S_{13}\Gamma_D \\ S_{31}\Gamma_G & (1 - S_{33}\Gamma_D) \end{vmatrix}}.$$

The above terms include the amplitude b_G of the generator wave; the scattering coefficients of the form $S_{i,j}$ of the three-arm waveguide junction representing the directional coupler, tuners, and waveguide section; and the reflection coefficients Γ_G , Γ_D , and Γ_L of the generator, detector, and load, respectively. The reflection coefficient Γ_{2i} is that of the equivalent generator as seen at the plane of the load.

The Γ_{2i} is obtained as follows: By assuming that $a_1 = b_1\Gamma_G$, $b_2 = a_2\Gamma_i$, $a_3 = b_3\Gamma_D$, and solving the scattering equations for a three-arm waveguide junction.

The scattering equations are

$$0 = -(1 - S_{11}\Gamma_G)b_1 + S_{12}a_2 + S_{13}\Gamma_D b_3,$$

$$b_2 = S_{21}\Gamma_G b_1 + S_{22}a_2 + S_{23}\Gamma_D b_3,$$

$$0 = S_{31}\Gamma_G b_1 + S_{32}a_2 - (1 - S_{33}\Gamma_D)b_3,$$

and the solution for Γ_{2i} using Cramer's rule is the expression shown above.

It is helpful to note that the above expression for K is closely related to the directivity

errata
→

$$D = 20 \log_{10} \left| \frac{S_{32}}{S_{31}} \right|. \quad (42)$$

One sees that for infinite directivity, $S_{31} = 0$, and $K = \infty$. Also if $\Gamma_{2i} = 0$, then (41) becomes

$$b_3 = \frac{S_{21}S_{32}b_G}{(1 - S_{11}\Gamma_G)(1 - S_{33}\Gamma_D)} \Gamma_L, \quad (43)$$

and the sidearm output level $|b_3|$ is proportional to $|\Gamma_L|$.

One can see how the tuning adjustments described above lead to this condition as follows: If Γ_L in (41) is the reflection coefficient of a sliding termination having a VSWR less than 1.02, then $|\Gamma_L| < 0.01$. With the tuning stubs withdrawn, one can say that $|\Gamma_{2i}| < 0.1$ and $|K| > 100$, for components easily obtainable. Thus $|\Gamma_{2i}\Gamma_L| < 0.001$, and $|K\Gamma_L| > 1$. Referring to (41) one sees that changes in phase of Γ_L caused by sliding the load will cause cyclical variations in $|b_3|$ mainly because of the numerator. It is also evident that these variations can be greatly reduced by increasing $|K|$, which can be effected by adjusting the tuner. When the variations have been reduced to ± 0.5 dB, then $|K|$ has been increased to approximately 3400.

The adjustment of the other tuner now proceeds after replacing the sliding termination by a sliding short-circuit. Note that $|\Gamma_L| \approx 1$, and $|K| = 3400$ in (41), while $|\Gamma_{2i}|$ is essentially unchanged. Thus $|K\Gamma_L| = 3400$ and $|\Gamma_{2i}\Gamma_L| < 0.1$. As the short-circuit slides, the variation in $|b_3|$ is now caused mainly by the denominator. Adjustment of the other tuner will affect Γ_{2i} without much effect on $|K|$ which is now large. When the variation in $|b_3|$ has been reduced to ± 0.02 dB, then $|\Gamma_{2i}| \approx 0.001$.

↳

The estimation of the above quantities $|K|$ and $|\Gamma_{2i}|$ from the residual variation in $|b_3|$ after the tuning process is stopped, is facilitated by the graphs of figures 17 and 18.

c. "Exact" Theory of Tuning Adjustments

While the approximate theory of the tuning adjustments is probably sufficient for most practical purposes, it may not suffice for the more critical experimenter, and a more exact theory is then of interest.

Assuming that (41) is sufficiently exact, the conditions for no cyclical

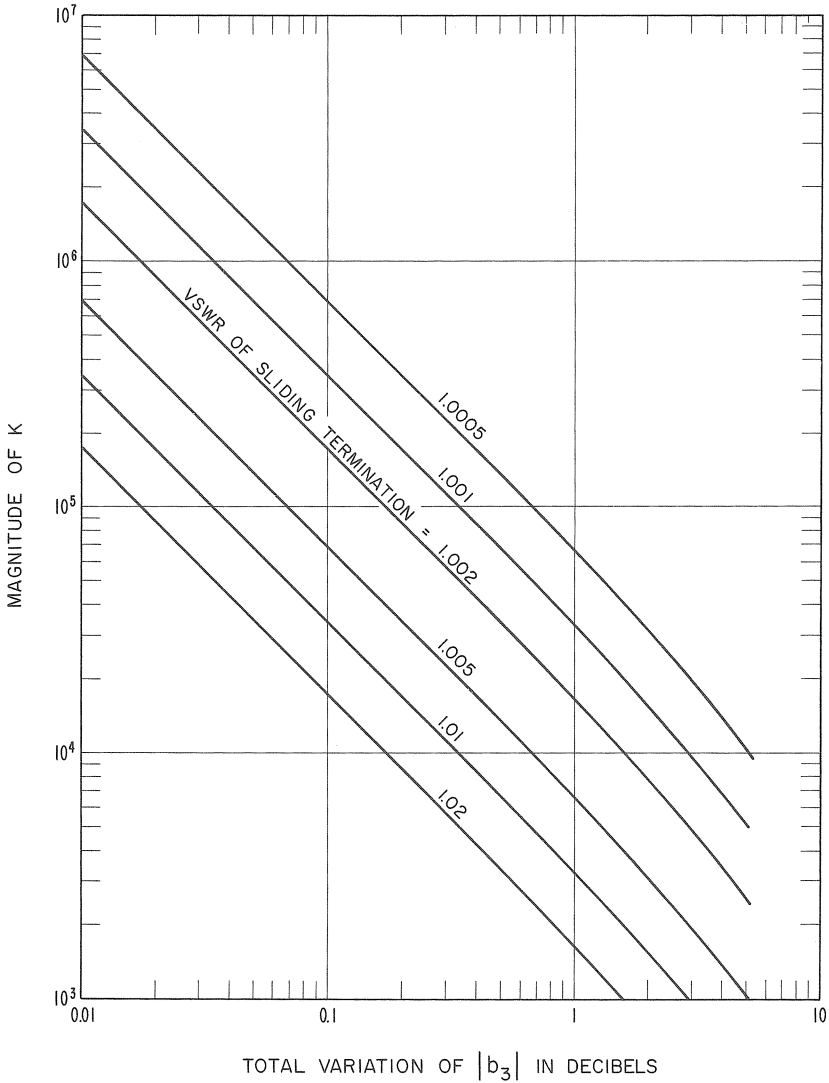


FIGURE 17. Graph showing effective directivity ratio K obtained in tuning process, versus the residual variation when tuning ceases, for sliding terminations having VSWR's from 1.0005 to 1.02.

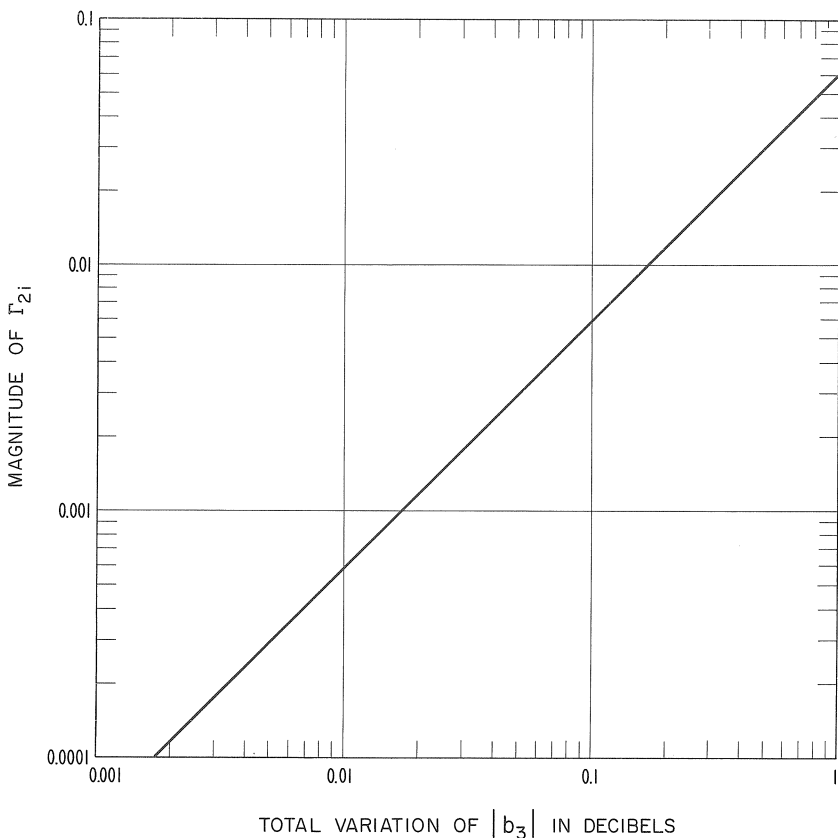


FIGURE 18. Graph showing magnitude of reflection coefficient of equivalent generator at terminal surface No. 2, versus residual variation when tuning ceases, for the sliding short-circuit termination.

variation of $|b_3|$ as we change the phase of Γ_L are as follows:

(1) $K = \infty, \Gamma_{2i} = 0$

(2) $\frac{1}{K\Gamma_L} = -\Gamma_{2i}^* \Gamma_L^*$

(3) $K = -\Gamma_{2i}$

(4) $\Gamma_L = 0$.

Although the first condition is the one finally desired, it is unlikely that we will obtain it in the first adjustment. We choose terminations for which $\Gamma_L \neq 0$ and avoid the fourth, while the third is an undesirable condition that would reduce $|K|$ rather than increase it, and is unlikely to result from normal adjustments of the tuners.

Thus the second condition is the one most likely to be obtained, or at least closely approached. If $|\Gamma_L| \approx 0.01$, and $|\Gamma_{2i}| \approx 0.1$, then condition (2) would require that $|K| = 10^5$. This might be the result of

adjusting the first tuner. Then if $|\Gamma_L|=1$, and $|K|=10^5$, condition (2) would require that $|\Gamma_{2i}|=10^{-5}$. This might be the result of adjusting the second tuner.

If a higher $|K|$ or lower $|\Gamma_{2i}|$ were then required, the adjustments could be repeated in sequence, although it seems probable that two or three adjustments would suffice for most purposes.

d. Error Analysis

Once $|K|$ and $|\Gamma_{2i}|$ are determined from the residual variations in $|b_3|$ after the tuning adjustments, the error in measuring the reflection coefficient $|\Gamma_u|$ of an unknown can be calculated. Curves are available [15] to determine limits of these error components directly from the residual variations in $|b_3|$. ← errata

In a typical example, the uncertainty in measuring $|\Gamma_u| \approx 0.2$ is less than 0.1 percent if the residual variation in $|b_3|$ is less than 0.5 dB when sliding a termination having a VSWR less than 1.01, and less than 0.02 dB when sliding a short-circuit. ← errata

In this case, errors from other sources are likely to be larger. Some of the other important sources of error are

(1) Error in measuring ratio of side arm outputs when substituting an unknown for a standard load. (This can be due to the error in the calibrated attenuator, if this technique is used.)

(2) Uncertainty caused by reflection from a waveguide joint or connector.

(3) Uncertainty in knowledge of the reflection coefficient $|\Gamma_S|$ of the standard load.

(4) Instabilities of source, detector, or other components.

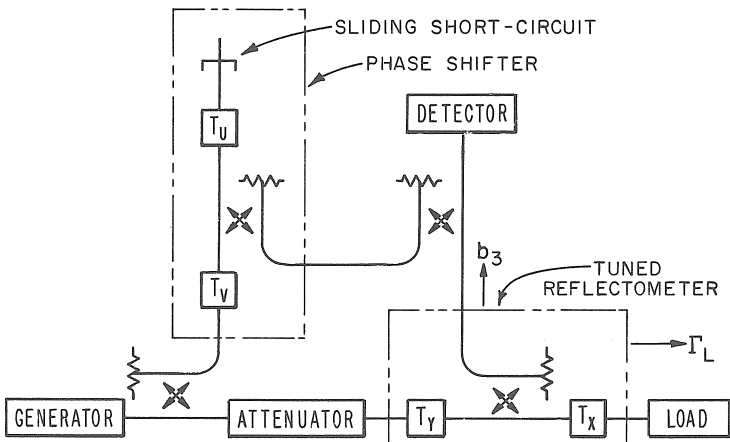


FIGURE 19. An arrangement for obtaining phase information with a reflectometer, using a sliding short-circuit and tuned directional coupler as a standard phase shifter. ← errata

10.4. Phase of Reflection Coefficient

A number of arrangements and techniques have been suggested for obtaining phase as well as amplitude information with reflectometers. One of these [16] is shown in the diagram of figure 19.

One adjusts both the attenuator and phase shifter to produce a detector output null. This is done alternately with the standard and the unknown connected at the plane of the load.

Ideally the difference in readings equals the difference in phase or amplitude, as the case may be.

A more refined version capable of greater accuracy is possible [17], but unless greater accuracy is really required, it would be well to avoid the tedious tuning operations required.

11. Reflection Coefficient Standards

In rectangular waveguide, many reflection coefficient standards have taken the form of waveguide discontinuities of simple geometry. The reflection is calculated from the geometry. Examples of these are the step in the narrow wall and the half-round inductive obstacle.

Most commercially available reflection coefficient standards employ a step in the narrow wall, making this occur at the waveguide joint, so that essentially a reduced height waveguide is joined to one having standard dimensions. The VSWR is, to a good approximation, equal to the ratio of the narrow wall inner dimensions, and is insensitive to frequency. There is a frequency-dependent, second-order correction for the discontinuity capacitance, but this is small if the reflection coefficient is 0.2 or less, which is usually the case. A sliding termination of small reflection usually is included, so that its effect on the total reflection can be taken into account and subtracted. Although these types of standards are convenient and have good accuracy and stability, there is no separation of the reflection from the discontinuity and that from the waveguide joint, and the effects of losses are neglected. Thus, more accurate standards can be constructed such as the half-round inductive obstacles.

The half-round inductive obstacle reflection coefficient standard [18, 19, 20] was designed to avoid sharp inside corners when electroformed, and accurate, calculated values are available. The reflection from the joint is separate, and nonstandard waveguide is not required. Corrections for finite conductivity of the metal are possible, but not yet available. The reflection from this type of standard is frequency sensitive.

Perhaps the most accurate reflection coefficient standard is the short-circuit, or more specifically, the quarter wavelength section of short-circuited waveguide [18]. This standard is frequency-sensitive, but is

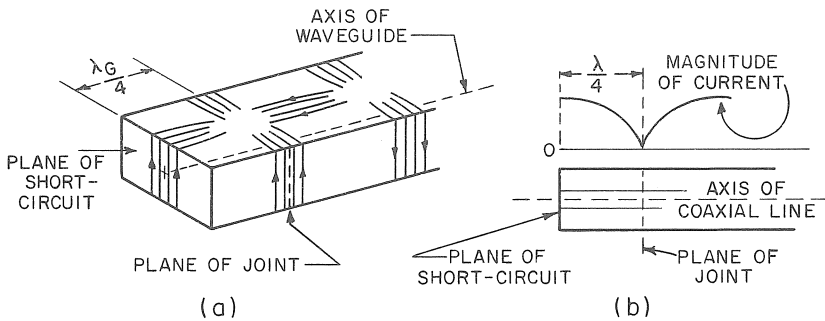


FIGURE 20. Diagrams showing current distribution in short-circuited sections of (a) rectangular waveguide ($TE_{1,0}$ mode), and (b) coaxial line.

not sensitive to small dimensional errors, or to reflections or losses at the waveguide joint. This freedom from losses at the joint is a result of the vanishing of the axial component of current at the joint, as shown in figure 20. Although the nominal reflection coefficient is unity, the actual reflection coefficient can be determined to very good accuracy from a knowledge of the microwave conductivity of the waveguide walls. These data are obtained from independent measurements. The actual reflection coefficient has also been determined by two other independent methods, giving close agreement. These methods are (1) measuring the Q of a cavity which incorporates the quarter wavelength reflection coefficient standard, and (2) measuring the losses of the standard by means of a microcalorimeter.

When using this type of standard to measure an unknown having a small reflection, the difference in return loss may be large, say 60 dB, and consequently difficult to measure accurately. However an adjustable load may be used as an intermediate source of reflections, making the measurement in two smaller steps, say 30 dB each.

In coaxial line, microwave reflection coefficient standards of the resistive type, have been constructed and also, the quarter wavelength short-circuit is used [16]. It is anticipated that further developments will be forthcoming now that a low reflection coaxial connector is generally available [21].

The present state of the art, regarding the accuracy of calibration of microwave standards of reflection coefficient at NBS, is described in an article [22] which is part of a series on high-frequency and microwave calibration services.

The constructive suggestions of Robert C. Powell, Bill C. Yates, and Harvey W. Lance of NBS for improving the presentation are gratefully acknowledged.

12. References

- [1] Additional theoretical background will be found in Basic Theory of Waveguide Junctions and Introductory Microwave Circuit Analysis, by David M. Kerns and Robert W. Beatty, to be published.
- [2] E. L. Ginzton, Microwave Measurements (McGraw-Hill Book Co., Inc., New York, N.Y., 1957), pp. 244-245.
- [3] W. Altar, P. Marshall, and L. Hunter, Probe error in standing-wave detectors, Proc. IRE **34**, No. 1, 33-44 (Jan. 1946).
- [4] A. C. MacPherson and D. M. Kerns, A new technique for the measurement of microwave standing-wave ratios, Proc. IRE **44**, No. 8, 1030 (Aug. 1956).
- [5] IT&T Corp., Reference Data for Radio Engineers, 4th ed. (New York, N.Y., 1957), p. 594.
- [6] S. Hopfer and L. Nadler, Waveguide rotary standing-wave indicators, PRD Repts. **6**, No. 1, 1-6 (Jan. 1959).
- [7] S. Hopfer and H. Finke, Impedance measurements in the 50-1000 Mc/sec range with a new standing-wave indicator, PRD Repts. **3**, No. 2, 1-7 (Jan. 1955).
- [8] E. L. Ginzton, Microwave Measurements (McGraw-Hill Book Co., Inc., New York, N.Y., 1957), p. 298.
- [9] R. A. Chipman, A resonance curve method for the absolute measurement of impedance at frequencies of the order of 300 Mc, J.A.P. **10**, 27-38 (Jan. 1939).
- [10] A. S. Meier and W. P. Summers, Measured impedance of vertical antennas over finite ground planes, Proc. IRE **37**, No. 6, 609-616 (June 1949).
- [11] R. W. Beatty, Magnified and squared VSWR responses for microwave reflection coefficient measurements, IRE Trans. Microwave Theory Tech. **MTT-7**, No. 3, 351-355 (July 1959).
- [12] G. F. Engen and R. W. Beatty, Microwave reflectometer techniques, IRE Trans. Microwave Theory Tech. **MTT-7**, No. 3, 351-355 (July 1959).
- [13] R. W. Beatty and W. J. Anson, Table of magnitude of reflection coefficient versus return loss ($L_R = 20 \log_{10} \frac{1}{|\Gamma|}$), NBS Tech. Note 72 (Sept. 19, 1960).
- [14] R. W. Beatty, Decibels return loss to magnitude of voltage reflection coefficient, Microwave Engineer's Handbook and Buyer's Guide, pp. TD188-192 (1961-62); pp. T221-225 (1963-64).
- [15] Wilbur J. Anson, A guide to the use of the modified reflectometer technique of VSWR measurement, J. Res. NBS **65C** (Eng. and Instr.), No. 4, 217-223 (Oct.-Dec. 1961).
- [16] R. W. Beatty and W. J. Anson, Application of reflectometer techniques to accurate reflection measurements in coaxial systems, Proc. IEE **109** (Pt. B), No. 46, 345-348 (July 1962).
- [17] R. W. Beatty, A microwave impedance meter capable of high accuracy, IRE Trans. Microwave Theory Tech. **MTT-8**, No. 4, 461-463 (July 1960).
- [18] R. W. Beatty and D. M. Kerns, Recently developed (Aug. 1958) microwave impedance standards and methods of measurement, IRE Trans. Instr. **1-7**, Nos. 3/4, 319-321 (Dec. 1958).
- [19] D. M. Kerns, Half-round inductive obstacles in rectangular waveguide, J. Res. NBS **64B** (Math. and Math. Phys.), No. 2, 113-130 (Apr.-June 1960).
- [20] Precision Measurement and Calibration—Electricity and Electronics, NBS Handb. **77**, Vol. 1 (Feb. 1, 1961).
- [21] A. E. Sanderson, A radically new coaxial connector for high-precision measurements, The General Radio Experimenter **37**, Nos. 2 and 3, pp. 1-6 (Feb.-Mar. 1963).
- [22] RSL Engineering Division (NBS), Microwave and high-frequency calibration services of the National Bureau of Standards—Reflection coefficient and immittance, IEEE Trans. Microwave Theory Tech. **MTT-12**, No. 6, correspondence (Nov. 1964).

errata
 →
 ↘

Additional References:

- [23] W.A. Wildhack, R.C. Powell, and H.L. Mason (Editors), "Accuracy in Measurements and Calibrations, 1965" NBS Technical Note 262, and R.C. Powell (Editor) "Accuracy in Electrical and Radio Measurements, NBS Technical Note 262-A.

U.S. GOVERNMENT PRINTING OFFICE : 1965 OL-767-763

National Bureau of Standards Monograph 82
Microwave Impedance Measurements and Standards

- ✓ p. 12 Add the following at the bottom of the page:

A simpler and more accurate expression for the limits of VSWR of σ_L , the VSWR of the load, is $\frac{\sigma}{\sigma_r} \geq \sigma_L \geq \sigma \sigma_r$, where σ is the VSWR observed in the slotted line, and σ_r is the residual VSWR. It is not required that $|\Gamma_r|$ be small for this expression to hold exactly in the lossless case. In the above example, this gives $2.40 \geq \sigma_L \geq 2.60$.

- ✓ p. 17 Fig. 10: Change Y_v to Y_u .

- ✓ p. 18 Immediately following Eq. (29): Change Y_v to Y_u .

Eq. (30): Change Y_v' to Y_u' .

Eq. (32): Change Γ_v' to Γ_u' .

- ✓ p. 24 Eq. (39): Change $|\Gamma_v|$ to $|\Gamma_u|$.

Eq. (40): Change $|\Gamma_v|$ to $|\Gamma_u|$.

Second line following Eq. (40): Change $|\Gamma_v|$ to $|\Gamma_u|$.

- ✓ p. 25 Line 11: Change "plane L." to "plane 1."

- ✓ p. 26 Eq. (42): Replace S_{32} in the numerator by $|S_{32}|$.

Next to last line: Change "as" to "is".

- ✓ p. 29 Section d., 3rd line: Change $|\Gamma_v|$ to $|\Gamma_u|$.

Section d., 6th line: Change $|\Gamma_v|$ to $|\Gamma_u|$.

Fig. 19: Close bottom of box around tuned reflectometer.

- ✓ Note additional references:

W. A. Wildhack, R. C. Powell, and H. L. Mason (Editors),

"Accuracy in Measurements and Calibrations, 1965"

NBS Technical Note 262, and R. C. Powell (Editor),

"Accuracy in Electrical and Radio Measurements, 1965"

NBS Technical Note 262-A.

2/14/66

Corrected by M. Binder USCOMM-ESSA-IER

U.S. DEPARTMENT OF COMMERCE
WASHINGTON, D.C. 20230

POSTAGE AND FEES PAID
U.S. DEPARTMENT OF COMMERCE

OFFICIAL BUSINESS
